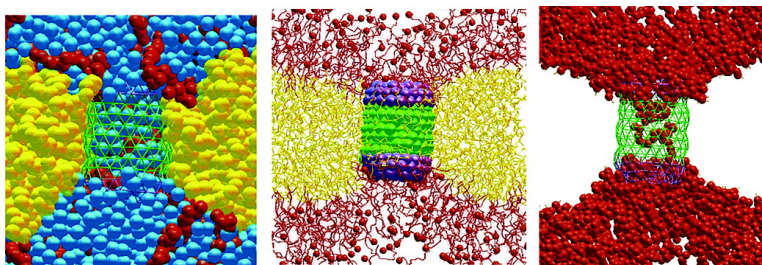


Key Roles for Chain Flexibility in Block Copolymer Membranes that Contain Pores or Make Tubes

Goundla Srinivas, Dennis E. Discher, and Michael L. Klein

Nano Lett., **2005**, 5 (12), 2343-2349 • DOI: 10.1021/nl051515x

Downloaded from <http://pubs.acs.org> on January 10, 2009



Key roles for chain flexibility in polymer bilayers

More About This Article

Additional resources and features associated with this article are available within the HTML version:

- Supporting Information
- Links to the 3 articles that cite this article, as of the time of this article download
- Access to high resolution figures
- Links to articles and content related to this article
- Copyright permission to reproduce figures and/or text from this article

[View the Full Text HTML](#)



NANO LETTERS

Key Roles for Chain Flexibility in Block Copolymer Membranes that Contain Pores or Make Tubes

Goundla Srinivas,^{†,§} Dennis E. Discher,^{‡,§} and Michael L. Klein^{*,†,§}

Center for Molecular Modeling, Department of Chemistry, Biophysical and Polymer Engineering Lab, Department of Chemical and Biomolecular Engineering, and Laboratory for Research on the Structure of Matter, University of Pennsylvania, Philadelphia, Pennsylvania 19104

Received August 2, 2005; Revised Manuscript Received September 13, 2005

ABSTRACT

Block copolymer amphiphiles that self-assemble into membranes present robust and functionalizable alternatives to biological assemblies. Coarse-grained molecular dynamics shows that thick bilayers of A–B copolymers accommodate protein-like channels and also tend to regulate transport. This occurs as flexible, hydrophilic A chains insert into the pore and obstruct water entry. A–B–A triblocks that exploit “hairpin” and “straight” conformations also show assembly into novel nanotubules and further highlight the key roles for chain flexibility in biomimetic block copolymer assemblies.

Despite considerable success in design, synthesis, and assembly of biomimetic polymer systems typified by polymer membranes,^{1–3} roles for molecular features such as polymer flexibility and chain conformation are still relatively unclear. Here, we begin to illustrate the effects and possibilities of flexibility and conformation by the use of coarse-grained (CG) molecular dynamics methodologies. We apply these novel simulation methods to two types of biomimetic membrane systems described recently: pores inserted into block copolymer membranes⁴ and tubes self-assembled from triblock copolymers.⁵

It is now well-established that block copolymer amphiphiles can be made lipid-like, which gives the copolymers their intrinsic ability to self-organize into membranes. Moreover, because a wide range of copolymer compositions and molecular weights (M_w) can be used and because increases in copolymer M_w lead to increases in membrane thickness up to 20 nm or more (versus 3–5 nm for lipid bilayers),⁶ these “polymersome” membrane systems considerably expand the range of membrane properties beyond those achievable with natural biomembranes.^{7–9} Properties that now seem tunable range from stability and rigidity to permeability and fluidity. Additionally, many biomembrane processes such as protein insertion, membrane fusion, DNA encapsulation ala' viruses, and compatibility have now been experimentally realized or mimicked in a range of synthetic

* Corresponding author. E-mail: klein@lrsm.upenn.edu.

† Center for Molecular Modeling, Department of Chemistry.

‡ Biophysical and Polymer Engineering Lab, Department of Chemical and Biomolecular Engineering.

§ Laboratory for Research on the Structure of Matter.

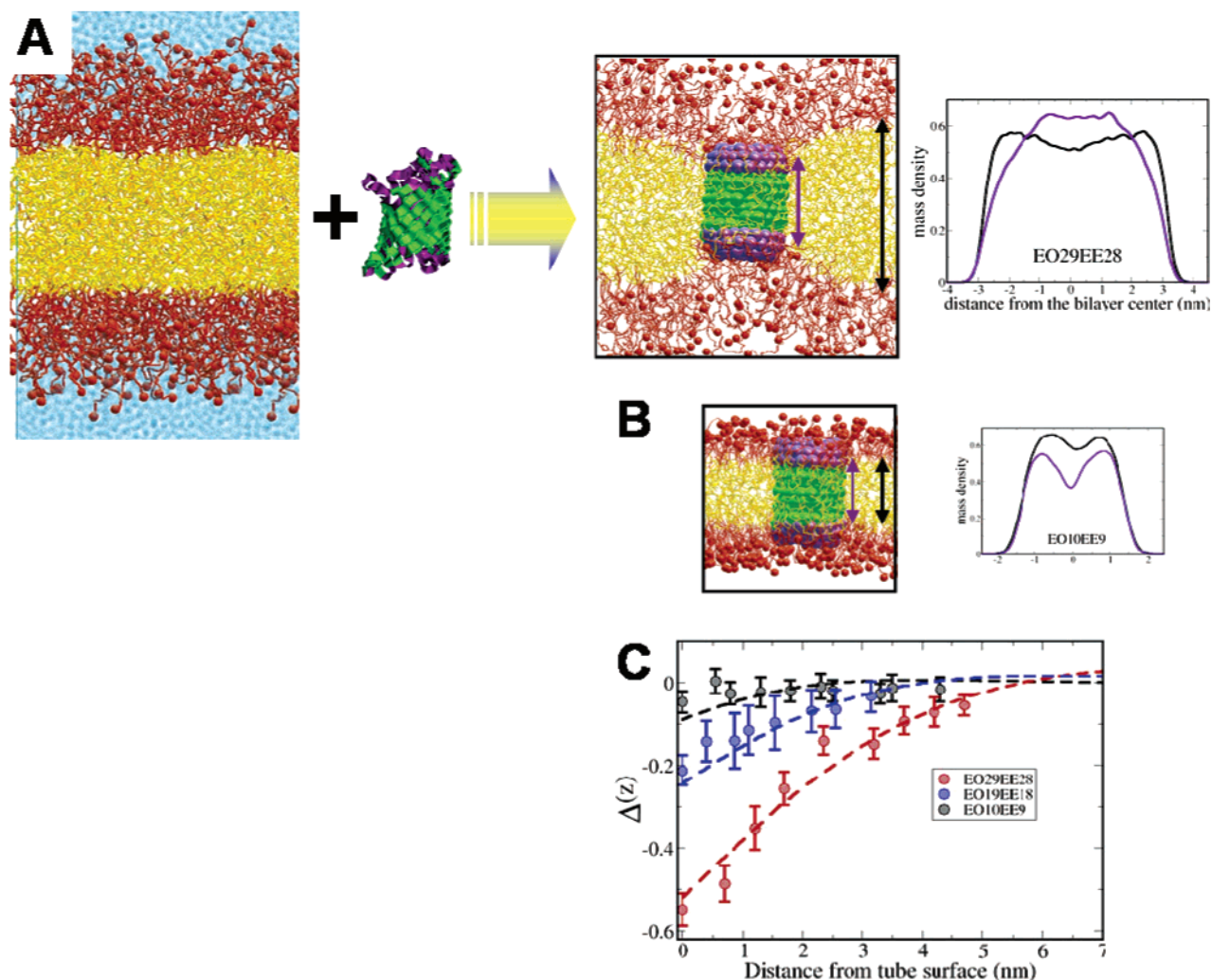


Figure 1. Self-assembled copolymer bilayer shown along with an OmpF membrane protein that is modeled as a porous cylinder with hydrophilic edges (purple). This is inserted into thicker (A) and thinner (B) polymer bilayers. PEO, PEE, and water are represented by red, yellow, and light blue, respectively. (C) Corresponding density distributions are shown both across the membrane and along the membrane interface. The latter compares favorably with theory.

polymer vesicle systems.^{8–10} The experimental successes bring to the fore questions about chain conformation and molecular-scale organization. In the case of inserting protein channels or pores that are matched in height to lipid bilayers but cannot span the unperturbed thickness of polymer membranes, questions arise regarding the very ability to insert a channel.^{11–13} Chain arrangements around the pore are also uncertain. Likewise, for tubules that self-assemble from triblock copolymers,⁵ the question arises as to whether the flexible chains take on predominantly membrane-spanning and/or U-shaped conformations.

Here, the perturbation of a protein-like channel inclusion on a biomimetic polymer membrane is illustrated by varying the thickness of the membrane. The role of chain flexibility on pore permeation is then studied in detail and suggests a novel mechanism for how polymer chains can regulate transport. In particular, we find that the water permeability coefficient shows a strong dependence on the polymer chain length. The CG simulations are then extended to study self-assembled tubular structures of *triblock* copolymers. In this second system, chain flexibility permits both membrane-

spanning and hairpin conformations of the chains, and the resulting distribution between these two states conforms to past theories.

Membrane proteins play a crucial role in cellular functions such as ion transport, ion regulation, energy transduction, and recognition. Despite such importance, very little is known about the structure and function of the membrane proteins for various reasons based on limited solubility. Functional materials and sensors¹⁴ based on these important gating structures are being pursued, but at least some of these systems prove to be lacking in robustness.¹⁵ It is clear from the few integral membrane protein structures solved to atomistic resolution that membrane proteins are surrounded by bounding lipids. Hence, the biophysical and biochemical properties of membrane proteins are determined by the lipid environment. Insertion and orientation follow a simple rule: the hydrophobic residues of pores bury inside the membrane core (lipid tail region), while the hydrophilic groups face the aqueous phase or line a pore. The same driving forces allow oriented insertion of model pores into synthetic polymer bilayers, as shown in Figure 1.

The membrane protein is modeled here as a hydrophobic cylinder with hydrophilic edges at the top and bottom. The thickness of the tube is selected so as to match the thickness of the smallest copolymer bilayer (EO₁₀EE₉) studied in this work. All of the other components present in the system, block copolymers and water, are represented by using a coarse-grained (CG) methodology. Each of the monomer units, ethyl ethylene (EE) and ethylene oxide (EO), are grouped into one single CG site, while three water molecules are grouped into a single CG water site. Most of the intermolecular potentials are of the simple Lennard-Jones form, while EO unit interaction is specified by a distance-dependent tabulated potential. The details of the coarse-grained procedure and the form of various potentials can be found in the Supporting Information and elsewhere.^{16,17} Simulations are carried out using an NPT ensemble at 298 K and a pressure of 1 atm with a 10 fs time step.

Simulations show that channel insertion leads to local bilayer deformation due to the “hydrophobic mismatch”.^{18–21} The amphiphile, whether lipid or polymer, within no more than one to two pore diameters of the inclusion responds in an effort to accommodate the inclusion. With polymer membranes, sustaining such perturbations is a consequence of both the flexibility and the stability of the copolymers and their assemblies. For lipids, the length of the lipid tails cannot be varied much and neither can the membrane thickness (~3–5 nm). Hence, one can only study with lipids the hydrophobic mismatch as a function of the protein thickness but not the other way around. On the other hand, biomimetic polymer membranes clearly provide a novel opportunity to explore the mismatch arising not just due to protein but also due to the membrane thickness which varies experimentally over a wide range (~3–30 nm). As shown by Smit et al.¹⁹ for the lipid bilayer, it is possible that the membrane protein may deform to mitigate the thickness mismatch. Nevertheless, in the present study, we have not considered the deformation of membrane protein.

In Figure 1, the effect of the inclusion channel on polymer bilayers of two different thicknesses is shown (EO₁₀EE₉ and EO₂₉EE₂₈ bilayers correspond to a thickness of 3 and 6 nm, respectively). The hydrophobic thickness of the EO₁₀EE₉ bilayer matches the inclusion thickness, and hence, the bilayer shows no deformation. On the other hand, EO₂₉EE₂₈ shows a strong negative mismatch. To further understand the insertion process, we have analyzed the density profiles for hydrophobic blocks both near and far from the inclusion. Upon insertion of the inclusion in the thinner EO₁₀EE₉ bilayer, the membrane becomes denser, but the bilayer shows little further sign of deformation. On the other hand, the EO₂₉EE₂₈ bilayer shows a symmetric deformation in both the upper and lower leaflets. Near the pore, the bilayer is denser as it is forced to wet the inserted, hydrophobic surface of the pore. The hydrophobic mismatch is 1.32 nm in this case, accounting for 22% of the bilayer thickness.

In simulations, we have calculated the thickness mismatch ($\Delta(z)$) as follows:

$$\Delta(z) = (d(z) - d_b)/d_b$$

where $d(z)$ and d_b correspond to the local thickness and the equilibrium bilayer thickness. The results are shown in Figure 1C. Dan et al.²² as well as others^{23,24} have theoretically determined expressions for the interfacial perturbation profile such as

$$\Delta(z) = (\Delta_0/2)(e^{i3/2A1/4z} + e^{-i3/2A1/4z}) \quad \text{and} \\ A = 16d_b N^2 \gamma^{(-4/3)}/a^5$$

Symmetric copolymers are assumed with the segment length and number of segments represented by a and N ($\sim M_w$). The interfacial tension at the hydrophobic/hydrophilic interface is represented by γ . The thickness mismatch obtained by using the above equation is also shown versus simulation results, and the two appear to be in good agreement. The range and extent of membrane deformation and thickness mismatch increase with increasing polymer length or bilayer thickness.

Note that lipids in biomembranes have limited flexibility and variation in length compared to copolymers. If copolymer bilayers cannot withstand the mismatch, the protein can be expelled from the bilayer. Because the lipid configurations of core tail are relatively limited, the lipid bilayers are relatively incompressible and cannot support large perturbations in thickness/surface density.²⁵ Even a small mismatch between the lipid bilayer and a transmembrane protein will therefore result in a large energetic penalty prohibiting protein incorporation. On the other hand, as explained by Dan et al.²² for self-assembled block copolymer bilayers, surface density is set by an energetic balance between the surface tension at the hydrophobic/hydrophilic interface and the additional degrees of freedom arising with chain conformations. The present simulation results show that the copolymer bilayer can withstand larger mismatches (>22%) in bilayer thickness as opposed to 2–3% in the case of lipid bilayers.^{22,25} This is in accordance with Dan et al.²² who predicted that a significant number of transmembrane proteins can be incorporated in block copolymer bilayers even with the large thickness mismatch. It may therefore be concluded that the greater the flexibility of the bilayer, the more conveniently the inclusion is accommodated.

Water penetration through the pore in the copolymer membranes depends on membrane thickness. In Figure 2A, the water penetration through a thin (EO₁₀EE₉) and a thick (EO₂₉EE₂₈) membrane is shown. Corresponding figures with the hydrophilic block of the copolymers and tube are shown in Figure 2B. As illustrated, copolymers perturb the water entry into the pore in both cases. For thick membranes, unsurprisingly, a significant length of polymer (typically two or more) is found inside the model pore. This increase in polymer concentration is accompanied by a decrease in water density inside the tube, as shown in Figure 2C, which plots the density profiles of water and poly(ethylene oxide) (PEO) as a function of distance from the tube center. The average density of water inside the tube is shown by a dashed line. For the membranes with longer copolymers, the water density decreases inside the tube while the corresponding PEO density increases.

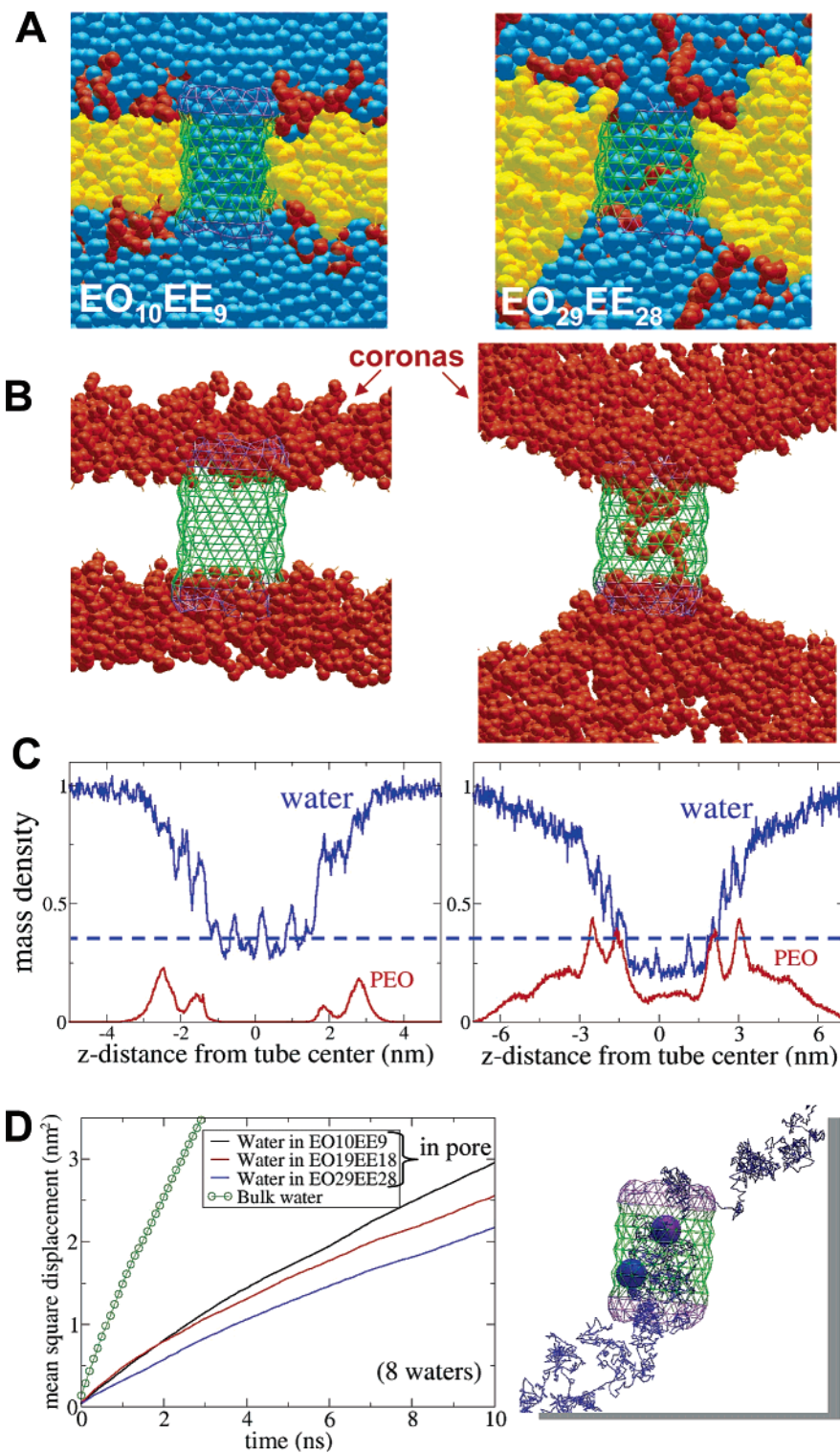


Figure 2. (A) Simulation snapshots of the water passage through the tube inserted in $EO_{10}EE_9$ and $EO_{29}EE_{28}$ bilayers. (B) Same as part A but without hydrophobic blocks and water. A PEO corona enters the tube in the case of the $EO_{29}EE_{28}$ bilayer and thus affects water permeation. (C) Density profiles of water and PEO inside the tube inserted in $EO_{10}EE_9$ and $EO_{29}EE_{28}$ bilayers. The dashed lines represent the average water density inside the tube. (D) Average mean square displacements (MSDs) of eight tagged waters inside the tube are plotted for three different cases. The water MSD is found to decrease with increasing bilayer thickness. For comparison, the MSD of bulk water is shown in the same figure. The trajectories of two water molecules inside the tube are also shown.

Diffusion of water within the tube and at the interface regions is also affected. Trajectories of two such water molecules are shown in Figure 2D along with the mean square displacement (MSD) curves for water in three different cases. For comparison, the MSD of bulk water is

also shown. As expected, the water diffuses much slower in the tube compared to bulk water. More interestingly, the self-diffusion in the tube decreases with increasing copolymer chain length. Hence, simulations suggest that the copolymer flexibility modulates channel transport function. It is not

difficult to imagine exploiting this phenomenon as a gating mechanism; for example, pores with some positive charge inside could be used to bind negative chains added to the copolymer membranes (e.g., poly(acrylic acid)–polybutadiene²⁶) and in a pH-dependent fashion.

To better understand the decreased self-diffusion of water in the pore, we have analyzed the membrane/inclusion interface in more detail. Snapshots corresponding to both thin and thick membranes are shown in Figure 3 A. For the thick membrane, the copolymer length is sufficiently long to partially obstruct the tube entrance. In Figure 3B, the densities of both PEO brushes and water in the selected regions over the tube (represented by broken cylinders) are plotted. The densities are preaveraged over a long run of 10 ns simulations and are shown as a function of distance z from the center of the inclusion. Note that with increasing PEO brush length the water penetration toward the membrane interface decreases. One unifying feature in all of the cases studied is the existence of a bottleneck in water–PEO densities, as shown in Figure 3B. The width of this bottleneck *decreases* with increasing PEO length, throttling or sieving the entry of water. In addition, the position of the bottleneck moves away from the inclusion surface as the PEO length increases (Figure 3B). Simulations reveal that, due to the negative hydrophobic mismatch, the EO density increases near the tube entrance, while it decreases to the same extent away from the surface (as explained in the Supporting Information). This reveals that the copolymers, being highly flexible, fall onto the tube entrance, thereby causing the density enhancement at the tube entrance. Note that the water displays complementary density profiles to those of EO. Hence, we conclude that the copolymer chain flexibility combined with the pronounced hydrophobic mismatch results in bottleneck-like density profiles for copolymers.

We have already shown that water diffusion inside the tube decreases with increasing membrane thickness. The water permeability coefficient (P_f) is related to its diffusion (D) by the following equation:²⁷

$$P_f = \phi D/d_{\text{pore}}$$

where d_{pore} denotes the pore length and, typically, $\phi = 1$. However, this does not account for the reduced probability of water entry into the pore—the corona filtration effect illustrated in Figures 2 and 3B. Integrating the latter density profiles to obtain the reduced volume fraction of water above the pore gives a correction of $\phi < 1$. The permeability coefficients obtained thus combine pore obstruction with corona filtration and are plotted in Figure 3C as a function of total copolymer mass (M_w).

When the membrane thickness matches the channel size, the permeation coefficient is insensitive to the membrane, but this maximum decreases nonlinearly with increasing membrane thickness, that is, increasing chain flexibility. Permeation coefficients for the range of simulated copolymers are fit reasonably well ($R^2 = 0.96$) to a saturable inhibition model:

$$\phi = \alpha - \alpha(M_w - M_0)/(M_1 + M_w)$$

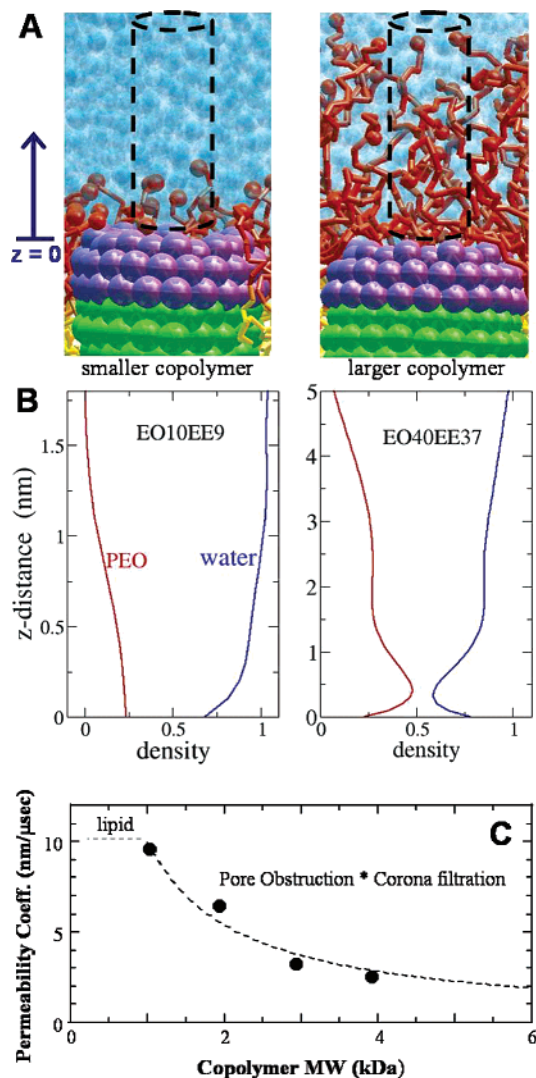


Figure 3. (A) Simulation snapshots shown along with the corresponding density profiles for the case of smaller (EO₁₀EE₉) and longer (EO₄₀EE₃₇) PEO lengths, revealing the effect of chain length on water penetration. Extrapolating the simulation results to the longer chain lengths reveals that in the case of longer polymers PEO brushes collapse onto the inclusion surface and thus prevent the water penetration by masking the inclusion. The cylindrical columns represent the configurational space in which the water densities are measured. (B) Density profiles of PEO (red) and water (blue) for two different copolymer lengths. Note that the extent of water penetration decreases with increasing PEO length. Also, the width of the bottleneck becomes increasingly narrower as the chain length increases. (C) The water permeability coefficient is plotted as a function of copolymer molecular weight (M_w). The symbols represent simulation results, while the dashed line is a fit to a permeability model that accounts for obstruction in the pore and corona filtration of water above it. The “lipid” region represents bilayers with channel-matching thickness.

where $M_0 = 0.97$ kDa, $\alpha D/d_{\text{pore}} = 10.2$ nm/μs, and $M_1 = 2.11$ kDa (see Figure 3C). The underlying basis for such a model is simple: flexible copolymer sterically obstructs or inhibits key water sites in and above the pore. Thus, this particular channel in a series of block copolymer membranes becomes nearly impermeable to water for $M_w \gg M_1$.

The simulation results above are in qualitative accord with recent experiments by Meier et al.,¹ who show significantly

reduced transport by pores in copolymer membranes. However, the longest copolymer ($\text{EO}_{40}\text{EE}_{37}$) studied in the simulations here is smaller than the experimental systems. By extrapolating the results here in Figure 3C, one finds that the copolymer systems studied in experiments indeed should have lower water permeation coefficients versus lipid bilayers. Simulations thus reveal that copolymer chain flexibility combined with hydrophobic mismatch can regulate water penetration across a copolymer bilayer.

Meier and co-workers⁴ recently showed that triblock copolymers form micrometer long tubules, which they termed “soft” tubes. In contrast to triblocks, diblock copolymers (both in experiment^{28–33} and simulation studies^{16,17}) lead to bilayers, wormlike micelles, and spherical micelles but not tubular structures. To further examine the role of chain flexibility, we have carried out CG simulations of self-assembly with $\text{EO}_4\text{EE}_{16}\text{EO}_4$ copolymers (EE/EO wt/wt ratio 2.54) that have qualitatively similar A–B–A triblock compositions to those of Meier et al.⁴ Final snapshots of triblock copolymer nanotubules are shown in Figure 4; cross-sectional views clearly show the water content present in the interior of the tube. While diblock copolymers could not produce such soft tube morphology over a wide range of compositions, the formation of stable tubular structures—up to 10 ns in simulation—seems especially characteristic of triblock copolymers.

Simulations reveal microscopic details on the structure and conformation of individual copolymers constituting the “tube”. We find that the copolymers adopt two major conformations, namely, (i) linear and (ii) hairpin or U conformations. In both conformations, hydrophilic blocks are exposed to aqueous regions, allowing the hydrophobic block to establish a core for the tube wall, as shown in Figure 4B. The inner and outer diameters of the tube respectively average 7.4 and 14.1 nm.

We have calculated the end-to-end distance and end–middle–end angle distributions of individual triblock copolymers in order to determine the individual conformations of copolymers inside the tube. The distributions (Figure 4B) are bimodal due to the linear plus hairpin conformations, although the hairpin conformations are predominant, as can be seen from the distributions. We find that there are 38% linear conformers present in the tube, which is in excellent agreement with recent experimental observations by Lodge and co-workers on copolymer melts.³⁴ Noting that the difference between the inner and outer radii of the tube is 3.8 nm, $\text{EO}_4\text{EE}_{16}\text{EO}_4$ can span this thickness and fully stretch itself only in a linear conformation. Hence, the polymers in the linear conformation are highly stretched and thus have an energetically unfavorable contribution to the resulting structure. On the other hand, polymers predominate in a relaxed hairpin conformation and thus have more freedom to explore the available configurational space. Thus, hairpin conformations are favored by energetic and entropic factors compared to linear conformations. Note that such microscopic details were largely inaccessible in experimental studies. Understanding such molecular level details will likely

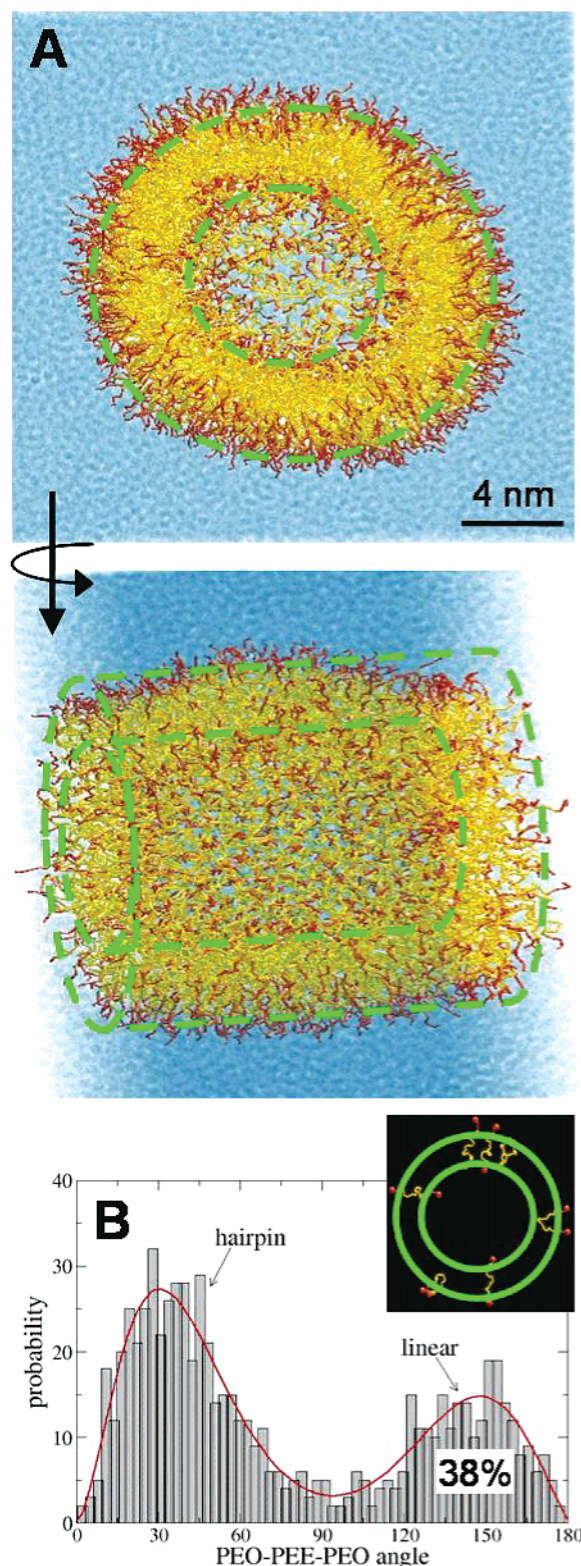


Figure 4. (A) Tubelike morphology obtained from $\text{EO}_4\text{EE}_{16}\text{EO}_4$ triblock copolymers. Both the cross-sectional and side views are shown. (B) Distribution PEO–PEE–PEO angle of triblock copolymers in a tube configuration are presented. The distribution reveals a predominant presence of the hairpin conformation of block copolymers in the tube. The inset shows a few representative linear and hairpin conformers present in the tube. Inner and outer shells of the soft tube are drawn as green circles.

be of great utility in further, rational design of biomimetic copolymer nanostructures.

In summary, computer simulations of chemistry-based, coarse-grained models offer novel insights into the key roles of flexibility in biohybrid synthetic materials. By studying both diblock and triblock copolymers, we have successfully obtained experimentally observed or theoretically predicted morphologies and added insight into corresponding structure and dynamics. In particular, by mimicking a membrane protein with a cylindrical pore, the effect of inclusion on PEO-PEE diblock copolymer membranes of different thicknesses is studied, revealing multifaceted roles of chain flexibility arising with hydrophobic mismatch. Highly flexible PEO chains enter and sterically mask the inclusion. Chain flexibility combined with hydrophobic mismatch thus has two important consequences: (i) accommodating the protein inclusions of various thicknesses and (ii) blocking water permeation of the pore. Analysis of individual water trajectories shows that the water diffusion inside the tube is slower than bulk water diffusion, contributing to a systematic decrease in the water permeation coefficient with increasing copolymer mass.

Triblock copolymers, in contrast to diblock copolymers, self-assemble into a tubelike structure, consistent with at least some experiments. Elaboration of individual copolymer conformations within the tube structure results in a bimodal distribution that reveals a majority of the copolymers in a hairpin conformation versus 38% linear conformers. This agrees with recent experiments.³⁴

Simulations with more realistic proteins and a wider range of copolymers and mixtures may provide further insight, but it is clear with inserted pores as well as copolymer tubes that chain flexibility can have important and probably useful roles in structure as well as function.

Acknowledgment. We thank NIH and NSF for their support and Steven Nielsen, Preston Moore, and John Shelley for their interest. We would like to thank Dr. Nily Dan and Veena Pata for the helpful discussions.

Supporting Information Available: Details of the coarse-grained model, interaction parameters, copolymer self-assembly, and simulation procedure. This material is available free of charge via the Internet at <http://pubs.acs.org>.

References

- (1) Taubert, A.; Napoli, A.; Meier, W. *Curr. Opin. Chem. Biol.* **2004**, *8*, 598–603.
- (2) Nardin, C.; Meier, W. *Chimia* **2001**, *55*, 142.
- (3) Sowadski, J. M. *J. Bioenerg. Biomembr.* **1996**, *28*, 3–5.
- (4) Grumelard, J.; Taubert, A.; Meier, W. *Chem. Commun.* **2004**, 1462–1463.
- (5) Stoescu, R.; Graff, A.; Meier, W. *Macromol. Biosci.* **2004**, *4*, 930–935.
- (6) Bermudez, H.; Brannan, A. K.; Hammer, D. A.; Bates, F. S.; Discher, D. E. *Macromolecules* **2002**, *35*, 8203–8208.
- (7) Meier, W.; Nardin, C.; Winterhalter, M. *Angew. Chem., Int. Ed.* **2000**, *39*, 4599–4602.
- (8) Ruyscharet, T.; Germain, M.; Gomes, J. F. P.; Fournier, D.; Sukhorukov, G. B.; Meier, W.; Winterhalter, M. *IEEE Trans. Biosci.* **2004**, *3*, 49–55.
- (9) Nardin, C.; Hirt, T.; Leukel, J.; Meier, W. *Langmuir* **2000**, *16*, 1035.
- (10) Bowie, J. U. *Curr. Opin. Struct. Biol.* **2000**, *10*, 435–437.
- (11) Dan, N.; Pincus, P.; Safran, S. A. *Langmuir* **1993**, *9*, 2768.
- (12) Dan, N.; Safran, S. A. *Isr. J. Chem.* **1995**, *35*, 37.
- (13) Dan, N.; Safran, S. A. *Biophys. J.* **1998**, *74*, 1410.
- (14) Georganopoulou, D.; Chang, L.; Nam, J.-M.; Thaxton, C. S.; Mufson, E. J.; Klein, W. L.; Mirkin, C. A. *Proc. Natl. Acad. Sci. U.S.A.* **2005**, *102*, 2273.
- (15) Rosi, N. L.; Mirkin, C. A. *Chem. Rev.* **2005**, *105*, 1547.
- (16) Srinivas, G.; Discher, D. E.; Klein, M. L. *Nat. Mater.* **2004**, *3*, 638.
- (17) Srinivas, G.; Shelley, J. C.; Nielsen, S. O.; Discher, D. E.; Klein, M. L. *J. Phys. Chem. B* **2004**, *108*, 8153.
- (18) Duque, D.; Li, X.; Katsov, K.; Schick, M. *J. Chem. Phys.* **2002**, *116*, 10478.
- (19) Venturoli, M.; Smit, B.; Sperotto, M. *Biophys. J.* **2005**, *88*, 1778.
- (20) Nielsen, S. O.; Ensing, B.; Ortiz, V.; Moore, P. B.; Klein, M. L. *Biophys. J.* **2005**, *88*, 3822.
- (21) Bohinc, K.; Kralj-Iglic, V.; May, S. *J. Chem. Phys.* **2003**, *119*, 7435.
- (22) Pata, V.; Dan, N. *Biophys. J.* **2003**, *85*, 2111.
- (23) Zemel, A.; Ben-shaul, A.; May, S. *Eur. Biophys. J.* **2005**, *34*, 230.
- (24) Mbamala, E.; Ben-shaul, A.; May, S. *Biophys. J.* **2005**, *88*, 1702.
- (25) Gennis, R. B. *Biomembranes: Molecular structure and function*; Springer-Verlag: New York, 1989.
- (26) Geng, Y.; Ahmed, A.; Bashin, N.; Discher, D. E. *J. Phys. Chem. B* **2005**, *109*, 3772.
- (27) Tien, H. T.; Ottova-Leitmannova, A. *Membrane biophysics: As viewed from experimental bilayer lipid membranes*; Elsevier: Amsterdam, The Netherlands, 2000; pp 349–442.
- (28) Discher, B. M.; Won, Y. Y.; Ege, D. S.; Lee, J. C.-M.; Bates, F. S.; Discher, D. E.; Hammer, D. A. *Science* **1999**, *284*, 1143–1146.
- (29) Jain, S.; Bates, F. S. *Science* **2003**, *300*, 460.
- (30) Hillmayer, M. A.; Bates, F. S. *Macromolecules* **1996**, *29*, 6994–7002.
- (31) Discher, D. E.; Eisenberg, A. *Science* **2002**, *297*, 967–973.
- (32) Zhang, L.; Eisenberg, A. *Science* **1995**, *268*, 727.
- (33) Hamley, I. W. *Nanotechnology* **2003**, *14*, R39–R54.
- (34) Schulze, J. S.; Moon, B.; Lodge, T. P.; Macosko, C. W. *Macromolecules* **2001**, *34*, 200.

NL051515X